

**TITLE PAGE**

**Role of Sphingolipid Mediator Ceramide in Obesity and Renal Injury in  
Mice Fed a High Fat Diet**

Krishna M. Boini, Chun Zhang, Min Xia, Justin L. Poklis, Pin-Lan Li

Department of Pharmacology and Toxicology, Medical College of Virginia Campus, Virginia  
Commonwealth University, Richmond, VA, 23298, USA

## **RUNNING TITLE PAGE**

**Running Title:** Ceramide in high fat diet-induced obesity

### **Address for correspondence:**

Pin-Lan Li, MD, PhD  
Department of Pharmacology and Toxicology  
Medical College of Virginia Campus  
Virginia Commonwealth University  
410 N, 12<sup>th</sup> Street, Richmond, VA, 23298  
Phone : (804) 828 4793  
Fax: (804) 828 4794  
E-mail: [pli@vcu.edu](mailto:pli@vcu.edu)

Number of text pages: 28

Number of figures: 7

Number of Tables: 1

Number of references: 32

Number of word count in abstract: 242

Number of word count in introduction: 494

Number of word count in discussion: 1489

**List of nonstandard abbreviations :** LFD, low fat diet ; HFD, high fat diet;

Ami : amitriptyline; ASMase, acid sphingomyelinase.

**Recommended section assignment:** Gastrointestinal, Hepatic, Pulmonary and Renal

## ABSTRACT

The present study tested a hypothesis that excess accumulation of sphingolipid, ceramide and/or its metabolites contribute to the development of obesity and associated kidney damage. LC/MS spectroscopy analysis demonstrated that C57BL/6J mice on the high fat diet (HFD) had significantly increased plasma total ceramide levels compared to the low fat diet (LFD)-fed animals. Treatment of mice with an acid sphingomyelinase (ASMase) inhibitor, amitriptyline, significantly attenuated the HFD-induced plasma ceramide levels. Corresponding to increase in plasma ceramide, the HFD significantly increased the body weight gain, plasma leptin concentration, urinary total protein and albumin excretion, glomerular damage index and adipose tissue ASMase activity compared to the LFD fed mice. These HFD-induced changes were also significantly attenuated by treatment of mice with amitriptyline. In addition, the decline of plasma glucose concentration following an intraperitoneal injection of insulin (0.15 U/kg B.W.) was more sustained in mice on the HFD with amitriptyline than on the HFD alone. Intraperitoneal injection of glucose (3 g/kg B.W.) resulted in a slow increase followed by a rapid decrease in the plasma glucose concentration in LFD and HFD plus amitriptyline treated mice, but such blood glucose response was not observed in HFD-fed mice. Immunofluorescence analysis demonstrated a decrease in the podocin and an increase in the desmin in the glomeruli of HFD-fed mice compared to the LFD and HFD plus amitriptyline treated mice. In conclusion, our results reveal a pivotal role for ceramide biosynthesis in obesity, metabolic syndrome and associated kidney damage.

## INTRODUCTION

Obesity has become a major global health concern and its incidence has increased sharply in the recent years. Obesity is one of the important criteria of the metabolic syndrome which is characterized by the concurrent existence of obesity, dyslipidemia, hyperglycemia, hyperinsulinemia and hypertension. It has been shown that obesity or metabolic syndrome is a strong and independent risk factor for cardiovascular disease that causes mortality (Lakka et al., 2002; Isomaa et al., 2001) and for the development of microalbuminuria and end-stage renal disease (Chen et al., 2004).

Recent evidence suggests that adipose tissue inflammation and abnormalities in sphingolipid metabolism may contribute to the metabolic and cardiovascular risk associated with obesity (Shah et al., 2008). Sphingolipids, such as ceramide, sphingosine, and sphingosine 1-phosphate, have been implicated in the pathogenesis of obesity, insulin resistance (Summers, 2006; Holland et al., 2007), and cardiovascular disease (Hojjati et al., 2005; Auge et al., 2000; Auge et al., 2004). Ceramide production is mediated by the hydrolysis of membrane sphingomyelin by acid sphingomyelinase (ASMase) or neutral sphingomyelinase (NSMase) or by *de novo* synthesis via serine palmitoyltransferase (SPT) and ceramide synthase (Futerman and Hannun, 2004). Ceramide is subsequently metabolized into sphingosine by ceramidases, and sphingosine can be further converted to S1P via sphingosine kinase (Futerman and Hannun, 2004) in response to a variety of mediators including proinflammatory cytokines, oxidative stress, and increased levels of free fatty acids. Ceramide and sphingosine inhibit insulin action and signaling in cultured cells (Summers, 2006). Inhibiting *de novo* ceramide synthesis prevented palmitate-mediated ceramide accumulation and inhibition of insulin signaling (Summers, 2006; Chavez et al., 2003; Powell

et al., 2004). Moreover, Holland *et al.* demonstrated that inhibition of ceramide synthesis by using the specific SPT inhibitor myriocin ameliorated obesity-induced insulin resistance. ASMase might play a role in obesity because it is over expressed in adipose tissue of ob/ob mice (Samad et al., 2006), and appears to be involved in the pathogenesis of atherosclerosis (Marathe et al., 1999), a disease which, similar to diabetes, is linked to obesity. More interestingly, a recent study has reported that high fat diet (HFD) increased the ceramide levels and ASMase expression in the adipose tissues and plasma from C57BL/6J mice (Shah et al., 2008). However, it remains unknown whether increased ASMase activity is involved in the development of obesity and associated glomerular injury or sclerosis.

The present study hypothesized that inhibition of ASMase may protect the HFD-induced obesity and associated glomerular injury and also improves the metabolic status in mice. To test this hypothesis, we performed a series of analyses in mice on high or low fat diet to determine whether inhibition of ASMase activity alters ceramide production, body weight gain and glomerular injury. Our results demonstrate that plasma ceramide may be a lipid mediator that contributes to the development of obesity and associated organ damage such as glomerular sclerosis. ASMase could be therapeutic target to reduce such lipid mediator in the plasma and to improve obesity-associated metabolic syndrome and end-stage organ damages.

## METHODS

**Animals:** Six weeks old male C57BL/6J mice were used in the present study (Jackson Laboratories, Bar Harbor, Maine). Mice were fed either a low fat diet (LFD: D 12450B, 10 kcal % fat, Research Diets, New Brunswick, NJ) or a high fat diet (HFD: D 12492, 60 kcal % fat, Research Diets, New Brunswick, NJ) with or without amitriptyline (Sigma, St. Louis, MO, USA) in the drinking water (AMI, 1 mM in drinking water (Brand et al., 2008)) for 13 weeks. All protocols were approved by the Institutional Animal Care and Use Committee of the Virginia Commonwealth University.

**Glucose tolerance and insulin tolerance test:** For determination of glucose tolerance, mice were fasted overnight and glucose (3 g/kg B.W.) was injected intraperitoneally (i.p.). Then, a drop of blood was drawn from the tail onto a test strip of a glucometer (Central Medical Incorporated, Eden Prairie, MN 55346) for measurement of blood glucose levels before and 15, 30, 45, 60, 75, 90, 120, 150, and 180 min after the injection. In another series of experiments, long-acting insulin (Novo Nordisk, Princeton, NJ) was injected (0.15 U/kg B.W., i.p.), and plasma glucose concentrations were determined at 0, 15, 30, 45, 60, and 90 min, as described above.

**Morphological examination:** The fixed kidneys were paraffin-embedded, and sections were prepared and stained with Periodic acid–Schiff stain. Glomerular damage index (GDI) was calculated from 0 to 4 on the basis of the degree of glomerulosclerosis and mesangial matrix expansion as described. In general, we counted 80-100 glomeruli in total in each kidney slice under microscope, when each glomerulus was graded level 0-4 damages. 0 represents no lesion, 1+ represents sclerosis of <25% of the glomerulus, while 2+, 3+, and 4+ represent

sclerosis of 25% to 50%, >50% to 75%, and >75% of the glomerulus. A whole kidney average sclerosis index was obtained by averaging scores from counted glomeruli (Zhang et al., 2010b). This observation was examined by three independent investigators who were blinded to the treatment of the experimental groups. The average of glomeruli score evaluated by the three investigators was reported.

**Acid sphingomyelinase (ASMase) activity:** The activity of ASMase was determined as we described previously (Yi et al., 2004). Briefly, *N*-methyl- $^{14}\text{C}$ -sphingomyelin was incubated with adipose tissue homogenates, and the metabolites of sphingomyelin,  $^{14}\text{C}$ -choline phosphate was quantified. An aliquot of homogenates (20  $\mu\text{g}$ ) was mixed with 0.02  $\mu\text{Ci}$  of *N*-methyl  $^{14}\text{C}$ -sphingomyelin in 100  $\mu\text{l}$  acidic reaction buffer containing 100 mmol/L sodium acetate, and 0.1% Triton X-100, pH 5.0, and incubated at 37°C for 15 min. The reaction was terminated by adding 1.5 ml chloroform:methanol (2:1) and 0.2 ml double-distilled water. The samples were then vortexed and centrifuged at 1,000  $g$  for 5 min to separate into two phases. A portion of the upper aqueous phase containing  $^{14}\text{C}$ -choline phosphate was transferred to scintillation vials and counted in a Beckman liquid scintillation counter. The choline phosphate formation rate ( $\text{nmol}\cdot\text{min}^{-1}\cdot\text{mg protein}^{-1}$ ) was calculated to represent the enzyme activity.

**Liquid chromatography–electrospray ionization tandem mass spectrometry (LC-ESI-MSMS) for quantitation of ceramide:** Separation, identification and quantitation of ceramide in plasma were performed by LC/MS. The HPLC equipped with a binary pump, a vacuum degasser, a thermostated column compartment and an autosampler (Waters, Milford, MA, USA). The HPLC separations were performed at 70°C on a RP C18 Nucleosil AB column (5  $\mu\text{m}$ , 70 mm x 2 mm i.d.) from Macherey Nagel (Düren, Germany). The mobile

phase was a gradient mixture formed as described (Fillet et al., 2002). The plasma lipids were extracted according to previous studies. To avoid any loss of lipids, the whole procedure was performed in siliconized glassware. MS detection was carried out using a Quattro II quadrupole mass spectrometer (Micromass, Altrincham, England) operating under MassLynx 3.5 and configured with a Z-spray electrospray ionization source. Source conditions were described as previously (Fillet et al., 2002).

**Histological Analysis of adipose tissue:** Adipose tissues were removed from the mice after 13 weeks on respective HFD or LFD with or without amitriptyline treatment. Formalin fixed, paraffin-embedded sections (6  $\mu$ m) were cut and stained with hematoxylin and eosin.

**Monitoring of arterial blood pressure in conscious mice:** Mean arterial pressure (MAP) was measured 12 weeks after mice were treated with the LFD or HFD as we described previously (Li et al., 2008). In brief, mice were anesthetized by inhalation of isoflurane, and then a catheter connected to a telemetry transmitter was implanted into the carotid artery and the transmitter was placed subcutaneously. The arterial blood pressure signal from the transmitter was received by a remote receiver and then recorded by a computer program (Data Sciences International, St. Paul, MN). Arterial blood pressure was continuously measured for one week after an equilibration period.

**Urinary total protein and albumin excretion measurement:** The 24-hour urine samples were collected using metabolic cages and subjected to total protein and albumin excretion measurements, respectively. Total protein content in the urine was detected by Bradford method using a UV spectrophotometer. Urine albumin was detected using a commercially available mouse albumin ELISA kit (Bethyl Laboratories, Montgomery, TX).



**Plasma leptin measurement:** Plasma concentrations of leptin were determined using enzyme linked immunoassay kit (Linco, St. Charles, USA).

**Real-time reverse transcription polymerase chain reaction (RT-PCR):** Total RNA from isolated mouse adipose tissue was extracted using TRIzol reagent (Invitrogen, Carlsbad, CA) according to the protocol as described by the manufacturer. RNA samples were quantified by measurement of optic absorbance at 260 nm and 280 nm in a spectrophotometer. The concentrations of RNA were calculated according to A260. Aliquots of total RNA (1 µg) from each sample were reverse-transcribed into cDNA according to the instructions of the first strand cDNA synthesis kit manufacturer (Bio-Rad, Hercules, CA). Equal amounts of the reverse transcriptional products were subjected to PCR amplification using SYBR Green as the fluorescence indicator on a Bio-Rad iCycler system (Bio-Rad, Hercules, CA). The primers used in this study were synthesized by Operon (Huntsville, AL) and the sequences were: ASM sense CACGTGGATGAGTTTGAGGT, antisense AGAGCTCCCAGAGTAGTTAC;  $\beta$ -actin sense TCGCTGCGCTGGTCGTC, antisense GGCCTCGTCACCCACATAGGA. The mRNA levels of the target gene were normalized to the  $\beta$ -actin mRNA levels detected from the same samples (Zhang et al., 2010a).

**Immunofluorescent staining:** Immunofluorescent staining was performed using frozen slides of mouse kidneys. After fixation with acetone, the slides were incubated with anti-podocin (Sigma, St. Louis, MO, USA, 1: 100) or anti-desmin (BD Biosciences, San Jose, CA, 1: 50) antibodies overnight at 4 °C. Then slides were washed and incubated with corresponding Texas Red-labeled secondary antibodies. Finally, the slides were washed, mounted and subjected to fluorescent microscopy examination. The images were captured

with a spot CCD camera (Diagnostic Instruments Inc., Sterlin Heights, MI, USA). All exposure settings were kept constant for each group of kidneys.

**Statistical Analysis:** Data are provided as arithmetic means  $\pm$  SEM,  $n$  represents the number of independent experiments. All data were tested for significance using ANOVA, paired or unpaired Student t-test as applicable. The glomerular damage index was analysed using a nonparametric Mann-Whitney rank sum test. Only results with  $p < 0.05$  were considered statistically significant.

## RESULTS

As illustrated in Fig. 1, HFD significantly increased the body weight of mice compared to LFD from week 3 in a time dependent manner. Surprisingly, ASMase inhibitor amitriptyline treatment attenuated the HFD-induced increase in the body weight. However, amitriptyline alone had no effect on the body weight during the treatment period in LFD fed mice. These data demonstrate that obesity was induced in our HFD fed mouse model. To further test whether ASMase inhibitor amitriptyline has similar effect in obese mice, the C57BL/6J mice were fed HFD for 11 weeks. After induction of obesity, the mice were further treated with amitriptyline for 2 weeks. HFD treatment significantly increased the body weight. However, treatment of mice with amitriptyline significantly decreased the body weight in these obese mice (Supplemental Figure 1).

Sphingolipids, such as ceramide, have been implicated in the pathogenesis of obesity. To test this possibility, we determined the effect of HFD on plasma ceramide levels in C57BL/6J WT mice. In response to the HFD, total plasma ceramide levels were significantly ( $p < 0.01$ ) increased in WT mice compared with LFD fed mice (Fig. 2A and Table 1), and the most abundant isoform is C24. However, additional treatment with amitriptyline, an inhibitor of ASMase significantly decreased the HFD-induced ceramide production (Fig. 2A and Table 1). This action of amitriptyline to decrease plasma ceramide level may be translated into the magnitude of downstream effects on weight gain metabolism, gene expression, insulin signaling, glomerular injury and leptin resistance. As illustrated in Fig. 2B, decreased plasma ceramide level significantly attenuated HFD-induced body weight gain. At the end of the feeding regime, the mice on the HFD gained  $19.1 \pm 1.3$  g, body weight where as mice on the LFD gained only  $7.8 \pm 0.7$  g. Amitriptyline treatment significantly attenuated the HFD

induced body weight gain ( $12.3 \pm 0.4$  g). Hematoxylin and eosin sections of adipose tissues showed that adipocyte size decreased in amitriptyline-treated HFD mice than in untreated HFD mice (Fig. 2C). Mean arterial pressure was similar in LFD or HFD-fed mice with or without amitriptyline treatment (Fig. 2D). These data reveal that the HFD-induced ceramide increase has effect on the body weight, but not on the mean arterial pressure. The gain of the body weight was not due to increased food intake because the average food intake was similar in LFD and HFD fed mice with (LFD + Ami:  $134 \pm 7$  vs. HFD + Ami:  $110 \pm 16$  mg/g B.W.,  $n = 8-10$ ) or without amitriptyline treatment (LFD:  $108 \pm 5$  vs. HFD:  $97 \pm 9$  mg/g B.W.,  $n = 5-6$ ). In another series of experiments, we attempted to determine the time course of ceramide in HFD-fed mice. The plasma ceramide concentration was significantly enhanced after 5 weeks of HFD treatment. In parallel to the enhancement of ceramide production at week 5, the blood glucose levels were significantly increased in WT mice fed the HFD (Supplemental Figure 2).

Next, we tested whether inhibition of ASMase in obese mice leads to improved glucose tolerance and insulin sensitivity. Intraperitoneal injection of glucose (3 g/kg B.W.) caused a slow increase followed by a rapid decrease in the plasma glucose concentrations in mice on the LFD and HFD with amitriptyline treatment. However, such blood glucose response was not observed in mice with the HFD alone (Fig. 3A). To test the insulin sensitivity, insulin was also injected intraperitoneally and plasma glucose concentrations were determined. As illustrated in Fig. 3B, the decline of plasma glucose concentration following an intraperitoneal injection of insulin (0.15 U/kg B.W.) was more sustained in mice on the HFD with amitriptyline than untreated HFD-fed mice, suggesting that an insulin sensitivity of cellular glucose uptake increases upon amitriptyline treatment in HFD mice.

Furthermore, we determined whether inhibition of ASMase contributes to the HFD-induced glomerular injury. As shown in Fig. 4, the HFD significantly increased the urinary total protein and albumin excretion compared to LFD-fed mice. Treatment with amitriptyline in HFD fed mice significantly attenuated HFD-induced urinary total protein and albumin excretion. However, amitriptyline had no effect on proteinuria and albuminuria in LFD-fed mice. Morphological analysis showed a typical pathological change in glomerular sclerotic damage, showing expanded glomerular mesangium with hypercellularity, capillary collapse and fibrous deposition in HFD fed mice. The average glomerular damage index was significantly higher in HFD fed mice compared to LFD fed mice. Treatment with amitriptyline attenuated these HFD-induced glomerular injuries (Fig. 4). Immunofluorescent analysis showed that desmin staining was more pronounced in glomeruli of HFD fed mice than in LFD fed mice. Desmin is an intermediate filament protein and has been suggested as an injured podocyte marker, the expression of which is often up-regulated in various glomerular diseases, in which podocyte damage is involved (Zhang et al., 2010b). Amitriptyline treatment decreased the HFD-induced elevation of desmin staining (Fig. 5A). However, another podocyte marker, podocin was markedly reduced in HFD fed glomeruli compared to those in LFD fed mice. Amitriptyline treatment almost completely attenuated the decrease in podocin staining (Fig. 5B).

To further explore the mechanism by which metabolic syndrome occurs in obese animals, we examined whether leptin resistance happens in HFD fed mice and whether the inhibition of ASMase changes leptin resistance in these animals. Leptin is released from adipocytes, and plasma leptin concentrations increase with adipocyte mass. Indeed, we found that plasma leptin concentrations were significantly higher in mice fed with the HFD than LFD. When

mice were receiving amitriptyline, increases in plasma leptin concentrations in HFD fed mice were significantly attenuated (Fig. 6).

Finally, we examined how HFD increased the plasma ceramide levels in mice. As shown in Fig. 7A, adipose tissue ASM mRNA expression was significantly higher in HFD fed mice with or without amitriptyline treatment compared to LFD fed mice. Moreover, biochemical analysis showed that the HFD significantly increased the ASMase activity in adipose tissue. Treatment with amitriptyline such HFD-induced increases in the ASMase activity in adipose tissues was substantially suppressed (Fig. 7B).

## DISCUSSION

The present study reveals that plasma ceramide plays a mechanistic role in HFD-induced obesity, insulin resistance and associated renal injury. We demonstrated for the first time that HFD-induced increase in plasma ceramide level was attenuated with amitriptyline treatment, providing evidence for the contribution of ASMase in the advancement of obesity. Furthermore, our results suggest that decrease in ceramide synthesis in adipose tissue may be a possible mechanism contributing to the enhanced insulin sensitivity, decreased leptin resistance and improved glomerular injury. It appears that ceramide is an adipocyte-derived active lipid, which may serve as a sphingolipid mediator contributing to the development of obesity and corresponding organ damage such as glomerular injury.

By LC-ESI-MS analysis, plasma ceramide level was found significantly increased in HFD fed mice which was blocked when these animals were administrated ASMase inhibitor, amitriptyline. Profiling analysis of ceramide in plasma demonstrated that although C24 ceramide constituted the major ceramide components that practically determine total ceramide levels, the most dramatic changes in response to HFD were observed from less dominant ceramide isoforms in blood of mice. For example, C16 increased by 400%, C18 by 301%, and C20 or C22 by 320%. Such diversity in changes in individual ceramide species has been previously observed in various physiological and pathological conditions (Dobrzyn and Gorski, 2002; Koybasi et al., 2004). It has been suggested that changes in specific ceramide species rather than changes in total ceramide concentrations may be more important to specific pathological events, a concept now widely accepted (Shah et al., 2008). It was also found that increases in both total ceramide and specific ceramide species observed in the plasma of mice on the HFD were reduced with amitriptyline treatment, indicating that increased ceramide is derived from

ASMase. In light of these data, it is tempting to speculate that improvements in the metabolic profile such as reduced weight, improved insulin resistance, improved glomerular injury, leptin resistance and so on by amitriptyline treatment in HFD fed mice is mediated, at least in part, by the reduction of ceramide production through ASMase. Indeed, we found that the ASMase activity and ASMase mRNA expression in adipose tissues were significantly increased in HFD fed mice. Treatment with amitriptyline significantly attenuated such HFD-induced ASMase activity in adipose tissues. These results further confirm that HFD-induced increases in plasma ceramide level are mainly due to activation of ASMase.

It is interesting that the reduced plasma ceramide levels upon amitriptyline treatment was accompanied with decreased body weight in HFD fed mice, which demonstrate that the reduction of body weights in amitriptyline treated obese mice is indeed due to the decrease in endogenous production of ceramide. Therefore, increases in endogenous production of ceramide contribute to the development of obesity, which is not associated with changes in food intake but rather with an alternate mechanism such as an increase in metabolism. Furthermore, we studied the effect of amitriptyline treatment in mice which have already developed obesity. The C57BL/6J mice were fed the HFD for 11 weeks for the induction of obesity. Administration of amitriptyline for 2 weeks in these mice significantly decreased the body weight. This further supports our hypothesis that inhibition of ASMase protects the HFD induced obesity. Although there are evidences that long term HFD increased blood pressure in rats (Dobrian et al., 2001; Wang et al., 2003; Deutsch et al., 2009), our present study showed that mean arterial pressure was not different in mice fed HFD or amitriptyline treatment. However, the HFD for 12 weeks significantly increased the urinary total protein and albumin excretion, a marker of renal injury and inhibition of ceramide production with amitriptyline prevented such renal injury. This renal injury is independent of the elevation of



arterial blood pressure since HFD has no effect on arterial blood pressure. Taken together, these findings suggest that HFD induces obesity and related glomerular injury in the kidney due to enhanced ceramide production associated with ASMase activity.

As reported earlier (Huang et al., 2006) the HFD induces insulin resistance. Treatment with amitriptyline in HFD fed mice improved glucose tolerance and enhanced the hypoglycemic activity, suggesting an insulin sensitivity of cellular glucose uptake. The improvements in weight gain and insulin resistance upon treatment with amitriptyline in mice on the HFD were correlated strongly with decreased levels of plasma ceramide. This suggests that ceramide also contributes to the development of insulin resistance. In this regard, increasing evidence has now established a role for ceramide as an intermediate mechanism that links excess nutrients (*e.g.* saturated fatty acids) and inflammatory cytokines (*e.g.* TNF- $\alpha$ ) to the induction of insulin resistance. For example, *in vivo* inhibition of *de novo* ceramide synthesis in various rodent models of obesity (Holland et al., 2007) improved insulin resistance. Thus, the reduction of plasma ceramide observed upon treatment with amitriptyline is a critical mechanism protecting from the HFD-induced insulin resistance and subsequent onset of diabetes in mice. In addition, we also determined the changes in plasma leptin level in mice receiving HFD with and without treatment of amitriptyline. The rationale for these measurements is that a clear link between obesity and insulin resistance, inflammation, and plasma leptin has been reported (Dobrian et al., 2001; Imig, 2008; Knight et al., 2008; Koh et al., 2005; Neels and Olefsky, 2006). A major hallmark of leptin resistance is hyperleptinemia, increased food intake, and decreased metabolism (Friedman, 1998; Friedman and Halaas, 1998). The present study found that the plasma leptin levels were elevated in mice fed on HFD compared with mice fed on LFD. Treatment of these HFD fed mice with amitriptyline abolished the increase in plasma leptin level. This indicates that ASMase activation in HFD

fed mice may also be attributed to increased leptin production, which reflects obesity and metabolic status in these mice.

In previous studies, ceramide has been implicated in the regulation of kidney function. Earlier reports from our laboratory (Yi et al., 2004) demonstrated that ceramide contributes to the development of chronic glomerular injury associated with hyperhomocysteinemia. Inhibitors of de novo synthesis of ceramide prevented L-homocysteine-induced ceramide formation in mesangial cells and also in the kidney and attenuated glomerular injury and proteinuria (Yi et al., 2004). In this study, we demonstrate that decreased ceramide via ASMase may have a protective role in the glomerular injury associated with obesity. In agreement with a deterioration of proteinuria, histological examinations in this study also showed that the glomerular mesangium was expanded with glomerular hypercellularity, capillary collapse and fibrous deposition in HFD fed mice, which was attenuated significantly by amitriptyline treatment, providing further evidence that glomerular injury induced by the HFD may be blocked by ASMase inhibition and therefore this sphingomyelinase could be a target of therapeutic strategy for obesity and related end stage organ damage.

To explore the mechanism of glomerular injury during HFD, we observed changes in podocyte function in mice exposed to the HFD with and without treatment of amitriptyline. It has been well documented that podocyte loss and dysfunction occurs with the onset and magnitude of glomerulosclerosis. Since podocytes serve as the final barrier against urinary protein loss in the normal glomeruli, any change in podocyte structure and function may be intimately associated with proteinuria and consequent glomerular sclerosis (Li et al., 2008). The present study showed that podocin protein markedly decreased in HFD fed mice and amitriptyline treatment restored podocin expression to the level comparable to the LFD fed

mice. In addition, we found that desmin as an intermediate filament protein and a specific and sensitive podocyte injury marker increased in the glomeruli when mice received the HFD. This increased desmin expression in the glomeruli was attenuated in HFD fed mice receiving amitriptyline. These results support the view that HFD-induced obesity associated with increased ceramide production may result in glomerular injury. Given that amitriptyline treatment prevented both obesity and glomerular podocyte injury and consequent glomerular injury or sclerosis, it is possible that this protective action of ASMase inhibition may be due to deterioration of obesity and consequent protection of the kidney from sclerotic injury. However, our recent studies reported that ceramide serves as an intermediate pathogenic factor that directly mediates Hcys-induced podocyte injury and glomerular sclerosis through enhancement of local oxidative stress (Yi et al., 2004; Zhang et al., 2010a). It is possible that the role of ceramide in obesity-induced glomerular injury may be different from that in hyperhomocysteinemia because a circulatory ceramide is increased in obesity. However, the direct effect of ceramide as an intracellular signalling molecule implicating in glomerular podocyte injury and glomerular sclerosis may not be excluded.

In summary, the present study demonstrated that ASMase inhibitor, amitriptyline attenuated the HFD-induced obesity and obesity-associated renal injury. Our results suggest that increased ceramide production via ASMase during the HFD is one of the important pathogenic factors in the development of obesity and associated end-stage organ damages such as glomerular sclerosis. Targeting ASMase by inhibition of its activity may be a novel therapeutic strategy for treatment and prevention of obesity and associated metabolic disturbance and/or end-stage organ damages.

## References

- Auge N, Maupas-Schwalm F, Elbaz M, Thiers JC, Waysbort A, Itohara S, Krell HW, Salvayre R, and Negre-Salvayre A (2004) Role for matrix metalloproteinase-2 in oxidized low-density lipoprotein-induced activation of the sphingomyelin/ceramide pathway and smooth muscle cell proliferation. *Circulation* **110**:571-578.
- Auge N, Negre-Salvayre A, Salvayre R, and Levade T (2000) Sphingomyelin metabolites in vascular cell signaling and atherogenesis. *Prog Lipid Res* **39**:207-229.
- Brand V, Koka S, Lang C, Jendrossek V, Huber SM, Gulbins E, and Lang F (2008) Influence of amitriptyline on eryptosis, parasitemia and survival of Plasmodium berghei-infected mice. *Cell Physiol Biochem* **22**:405-412.
- Chavez JA, Knotts TA, Wang LP, Li G, Dobrowsky RT, Florant GL, and Summers SA (2003) A role for ceramide, but not diacylglycerol, in the antagonism of insulin signal transduction by saturated fatty acids. *J Biol Chem* **278**:10297-10303.
- Chen J, Muntner P, Hamm LL, Jones DW, Batuman V, Fonseca V, Whelton PK, and He J (2004) The metabolic syndrome and chronic kidney disease in U.S. adults. *Ann Intern Med* **140**:167-174.
- Deutsch C, Portik-Dobos V, Smith AD, Ergul A, and Dorrance AM (2009) Diet-induced obesity causes cerebral vessel remodeling and increases the damage caused by ischemic stroke. *Microvasc Res* **78**:100-106.
- Dobrian AD, Davies MJ, Schriver SD, Lauterio TJ, and Prewitt RL (2001) Oxidative stress in a rat model of obesity-induced hypertension. *Hypertension* **37**:554-560.
- Dobrzyn A and Gorski J (2002) Ceramides and sphingomyelins in skeletal muscles of the rat: content and composition. Effect of prolonged exercise. *Am J Physiol Endocrinol Metab* **282**:E277-E285.

- Fillet M, Van Heugen JC, Servais AC, De Graeve J, and Crommen J (2002) Separation, identification and quantitation of ceramides in human cancer cells by liquid chromatography-electrospray ionization tandem mass spectrometry. *J Chromatogr A* **949**:225-233.
- Friedman JM (1998) Leptin, leptin receptors, and the control of body weight. *Nutr Rev* **56**:s38-s46.
- Friedman JM and Halaas JL (1998) Leptin and the regulation of body weight in mammals. *Nature* **395**:763-770.
- Futerman AH and Hannun YA (2004) The complex life of simple sphingolipids. *EMBO Rep* **5**:777-782.
- Hojjati MR, Li Z, Zhou H, Tang S, Huan C, Ooi E, Lu S, and Jiang XC (2005) Effect of myriocin on plasma sphingolipid metabolism and atherosclerosis in apoE-deficient mice. *J Biol Chem* **280**:10284-10289.
- Holland WL, Brozinick JT, Wang LP, Hawkins ED, Sargent KM, Liu Y, Narra K, Hoehn KL, Knotts TA, Siesky A, Nelson DH, Karathanasis SK, Fontenot GK, Birnbaum MJ, and Summers SA (2007) Inhibition of ceramide synthesis ameliorates glucocorticoid-, saturated-fat-, and obesity-induced insulin resistance. *Cell Metab* **5**:167-179.
- Huang DY, Boini KM, Osswald H, Friedrich B, Artunc F, Ullrich S, Rajamanickam J, Palmada M, Wulff P, Kuhl D, Vallon V, and Lang F (2006) Resistance of mice lacking the serum- and glucocorticoid-inducible kinase SGK1 against salt-sensitive hypertension induced by a high-fat diet. *Am J Physiol Renal Physiol* **291**:F1264-F1273.
- Imig JD (2008) Eicosanoids and renal damage in cardiometabolic syndrome. *Expert Opin Drug Metab Toxicol* **4**:165-174.

- Isomaa B, Almgren P, Tuomi T, Forsen B, Lahti K, Nissen M, Taskinen MR, and Groop L (2001) Cardiovascular morbidity and mortality associated with the metabolic syndrome. *Diabetes Care* **24**:683-689.
- Knight SF, Quigley JE, Yuan J, Roy SS, Elmarakby A, and Imig JD (2008) Endothelial dysfunction and the development of renal injury in spontaneously hypertensive rats fed a high-fat diet. *Hypertension* **51**:352-359.
- Koh KK, Han SH, and Quon MJ (2005) Inflammatory markers and the metabolic syndrome: insights from therapeutic interventions. *J Am Coll Cardiol* **46**:1978-1985.
- Koybasi S, Senkal CE, Sundararaj K, Spassieva S, Bielawski J, Osta W, Day TA, Jiang JC, Jazwinski SM, Hannun YA, Obeid LM, and Ogretmen B (2004) Defects in cell growth regulation by C18:0-ceramide and longevity assurance gene 1 in human head and neck squamous cell carcinomas. *J Biol Chem* **279**:44311-44319.
- Lakka HM, Laaksonen DE, Lakka TA, Niskanen LK, Kumpusalo E, Tuomilehto J, and Salonen JT (2002) The metabolic syndrome and total and cardiovascular disease mortality in middle-aged men. *JAMA* **288**:2709-2716.
- Li N, Chen L, Yi F, Xia M, and Li PL (2008) Salt-sensitive hypertension induced by decoy of transcription factor hypoxia-inducible factor-1alpha in the renal medulla. *Circ Res* **102**:1101-1108.
- Marathe S, Kuriakose G, Williams KJ, and Tabas I (1999) Sphingomyelinase, an enzyme implicated in atherogenesis, is present in atherosclerotic lesions and binds to specific components of the subendothelial extracellular matrix. *Arterioscler Thromb Vasc Biol* **19**:2648-2658.
- Neels JG and Olefsky JM (2006) Inflamed fat: what starts the fire? *J Clin Invest* **116**:33-35.

- Powell DJ, Turban S, Gray A, Hajduch E, and Hundal HS (2004) Intracellular ceramide synthesis and protein kinase C $\zeta$  activation play an essential role in palmitate-induced insulin resistance in rat L6 skeletal muscle cells. *Biochem J* **382**:619-629.
- Samad F, Hester KD, Yang G, Hannun YA, and Bielawski J (2006) Altered adipose and plasma sphingolipid metabolism in obesity: a potential mechanism for cardiovascular and metabolic risk. *Diabetes* **55**:2579-2587.
- Shah C, Yang G, Lee I, Bielawski J, Hannun YA, and Samad F (2008) Protection from high fat diet-induced increase in ceramide in mice lacking plasminogen activator inhibitor 1. *J Biol Chem* **283**:13538-13548.
- Summers SA (2006) Ceramides in insulin resistance and lipotoxicity. *Prog Lipid Res* **45**:42-72.
- Wang MH, Smith A, Zhou Y, Chang HH, Lin S, Zhao X, Imig JD, and Dorrance AM (2003) Downregulation of renal CYP-derived eicosanoid synthesis in rats with diet-induced hypertension. *Hypertension* **42**:594-599.
- Yi F, Zhang AY, Janscha JL, Li PL, and Zou AP (2004) Homocysteine activates NADH/NADPH oxidase through ceramide-stimulated Rac GTPase activity in rat mesangial cells. *Kidney Int* **66**:1977-1987.
- Zhang C, Hu JJ, Xia M, Boini KM, Brimson C, and Li PL (2010a) Redox signaling via lipid raft clustering in homocysteine-induced injury of podocytes. *Biochim Biophys Acta* **1803**:482-491.
- Zhang C, Hu JJ, Xia M, Boini KM, Brimson CA, Laperle LA, and Li PL (2010b) Protection of podocytes from hyperhomocysteinemia-induced injury by deletion of the gp91phox gene. *Free Radic Biol Med* **48**:1109-1117.

## FOOTNOTES

This work was supported by the National Institutes of Health National Institute of Diabetes and Digestive and Kidney Diseases [Grant DK54927] and National Institutes of Health National Heart, Lung, and Blood Institute [Grant HL091464, HL57244].



## LEGENDS FOR FIGURES

### **Fig. 1. Effects of the low fat and high fat diet on body weight with or without amitriptyline treatment.**

A: Values are means  $\pm$  SE (n=10-12 each group) of body weight in LFD and HFD fed C57BL/6J mice with or without amitriptyline (Ami) treatment. \* Significant difference ( $P<0.05$ ) compared to the values from mice receiving the LFD, # Significant difference ( $P<0.05$ ) compared to the values from mice receiving the HFD.

### **Fig. 2. Plasma total ceramide concentrations, delta body weight, adipocyte size and arterial blood pressure in C57BL/6J mice on low fat or high fat diet with or without amitriptyline treatment.**

Data are arithmetic means  $\pm$  SE (n=4-12 each group) of plasma total ceramide concentrations (A), delta body weight (B), adipocyte size (original magnification, x100) (C) and mean arterial blood pressure (D) in LFD or HFD fed C57BL/6J mice with or without amitriptyline treatment. \* Significant difference ( $P<0.05$ ) compared to the values from mice receiving the LFD, # Significant difference ( $P<0.05$ ) compared to the values from mice receiving the HFD. Scale bar represents 50  $\mu$ m.

### **Fig. 3. Plasma glucose concentrations following intraperitoneal glucose or insulin injection in C57BL/6J mice on low fat or high fat diet with or without amitriptyline treatment.**

Values are arithmetic means  $\pm$  SE (n= 6 each group) of plasma glucose concentrations following intraperitoneal injection of glucose (3 g/kg B.W., A) or insulin (0.15 U/kg B.W., B) in LFD or HFD fed C57BL/6J mice with or without amitriptyline treatment. \* Significant

difference ( $P<0.05$ ) compared to the values from mice receiving the LFD, <sup>#</sup> Significant difference ( $P<0.05$ ) compared to the values from mice receiving the HFD.

**Fig. 4. Morphological features of the glomeruli in low fat or high fat diet treatment in C57BL/6J mice on low fat or high fat diet with or without amitriptyline treatment.**

**A:** Photomicrographs show typical glomerular structure (original magnification, x400) in LFD or HFD treatment with or without amitriptyline treatment. **B:** Summarized data of glomerular damage index (GDI) by semi-quantitation of scores in 4 different groups of mice (n=6 each group). For each kidney section, 50 glomeruli were randomly chosen for the calculation of GDI. **C:** Urinary total protein excretion, **D:** Urinary albumin excretion (n=6-10 each group). \* Significant difference ( $P<0.05$ ) compared to the values from mice receiving the LFD, # Significant difference ( $P<0.05$ ) compared to the values from mice receiving the HFD. Scale bar represents 50  $\mu$ m.

**Fig. 5. Immunofluorescent staining of desmin and podocin from C57BL/6J mice on low fat or high fat diet with or without amitriptyline treatment.**

**A:** Typical images of desmin staining in glomeruli from C57BL/6J mice on the LFD or HFD with or without amitriptyline treatment (n= 4 each group). **B:** Typical images of podocin staining in glomeruli from C57BL/6J mice on the LFD or HFD with or without amitriptyline treatment (n= 4 each group). Scale bar represents 20  $\mu$ m.

**Fig. 6. Plasma leptin concentrations.**

Values are arithmetic means  $\pm$  SEM (n=6 each group) of plasma leptin concentrations in LFD and HFD fed C57BL/6J mice with or without amitriptyline treatment. \* Significant difference

( $P < 0.05$ ) compared to the values from mice receiving the LFD, # Significant difference ( $P < 0.05$ ) compared to the values from mice receiving the HFD.

**Fig. 7. Effect of the low fat diet and high fat diet on adipose tissue ASMase mRNA expression and ASMase activity in C57BL/6J mice on low fat or high fat diet with or without amitriptyline treatment.**

Values are arithmetic means  $\pm$  SEM (n=6 each group) of ASMase mRNA expression (A) and ASMase activity (B) in LFD and HFD fed C57BL/6J mice with or without amitriptyline treatment.. \* Significant difference ( $P < 0.05$ ) compared to the values from mice receiving the LFD, # Significant difference ( $P < 0.05$ ) compared to the values from mice receiving the HFD.

**Table 1: Ceramide concentrations (ng/mg protein) in mice fed low fat or high fat diet with or without amitriptyline treatment measured by LC/MS spectrometry (n=4-6).**

Ceramide	LFD	LFD + Ami	HFD	HFD + Ami
C16	0.3 ± 0.1	0.4 ± 0.4	1.3 ± 1.0	0.3 ± 0.2
C18	0.5 ± 0.2	2.6 ± 2.6	1.6 ± 0.9	0.6 ± 0.2
C20	1.2 ± 0.2	1.7 ± 0.2	6.6 ± 1.1 <sup>*</sup>	4.0 ± 0.3 <sup>#</sup>
C22	9.7 ± 1.3	13.5 ± 3.5	31.5 ± 9.0 <sup>*</sup>	20.2 ± 4.2
C24	35.7 ± 9.8	27.7 ± 9.8	61.5 ± 1.5 <sup>*</sup>	46.6 ± 8.2
Total	47.4 ± 9.2	45.7 ± 5.8	102.5 ± 11.1 <sup>*</sup>	71.8 ± 8.3 <sup>#</sup>

LFD: Low fat diet; HFD: High fat diet; Ami: Amitriptyline. \* Significant difference ( $P < 0.05$ ) compared to the values from mice receiving the LFD, # Significant difference ( $P < 0.05$ ) compared to the values from mice receiving the HFD

**Fig. 1**

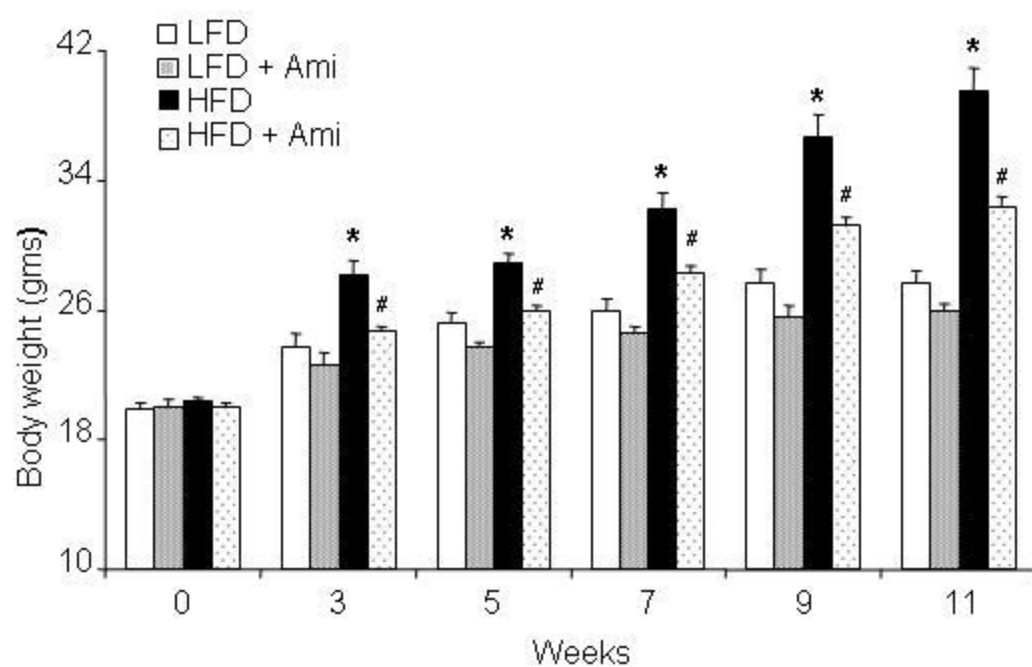


**Fig. 2**

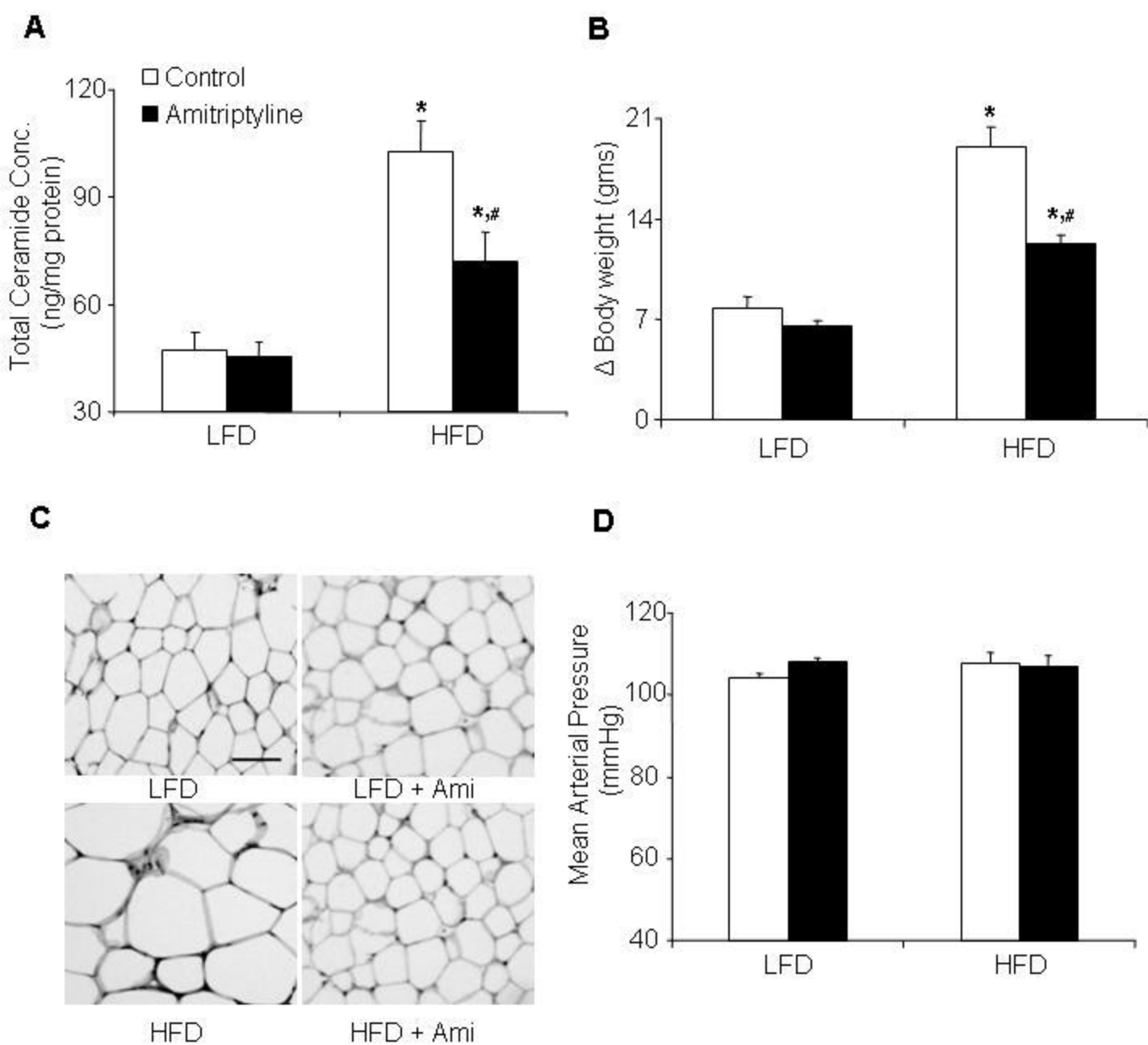
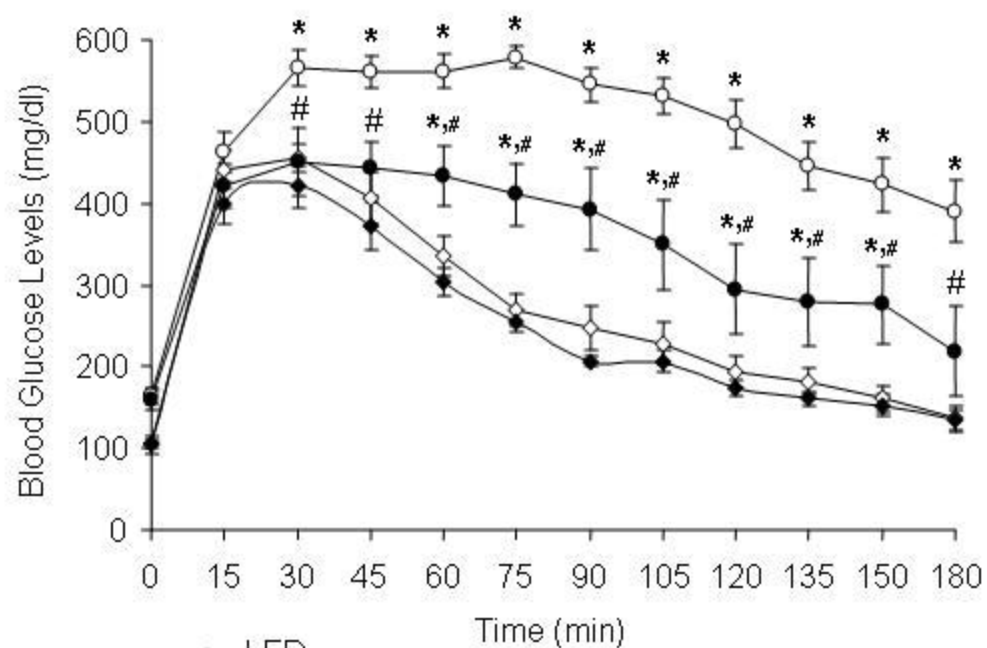


**Fig. 3**

**A**



**B**

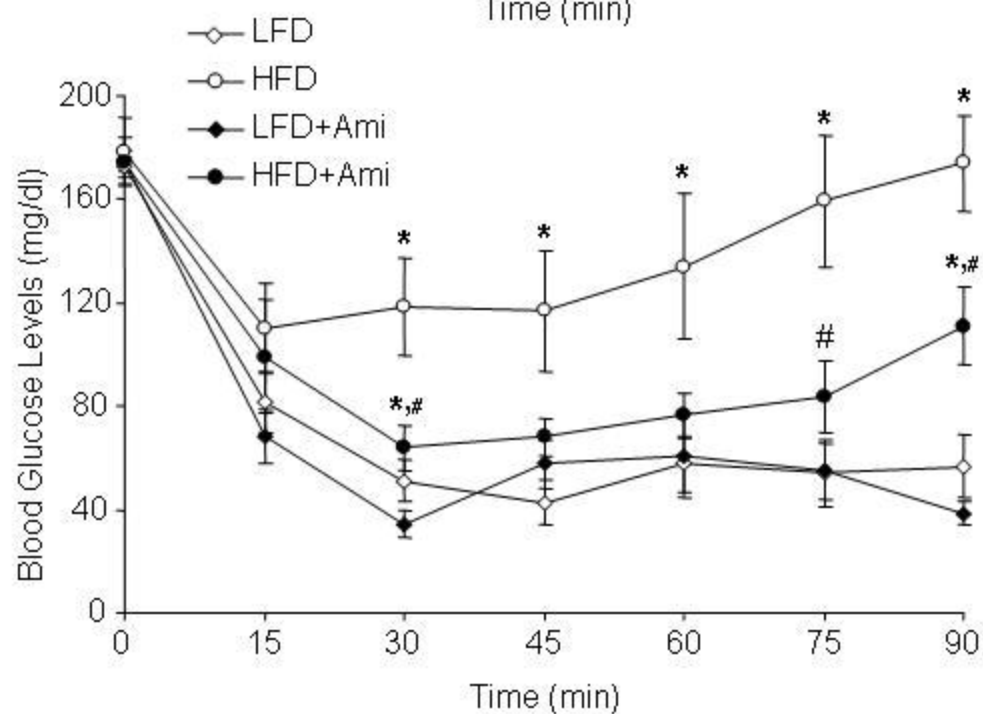
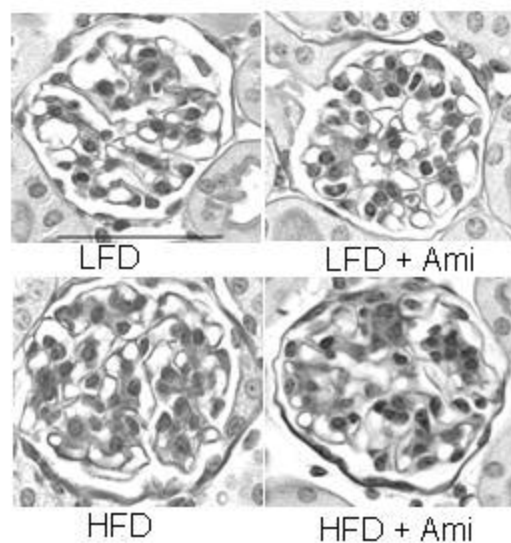
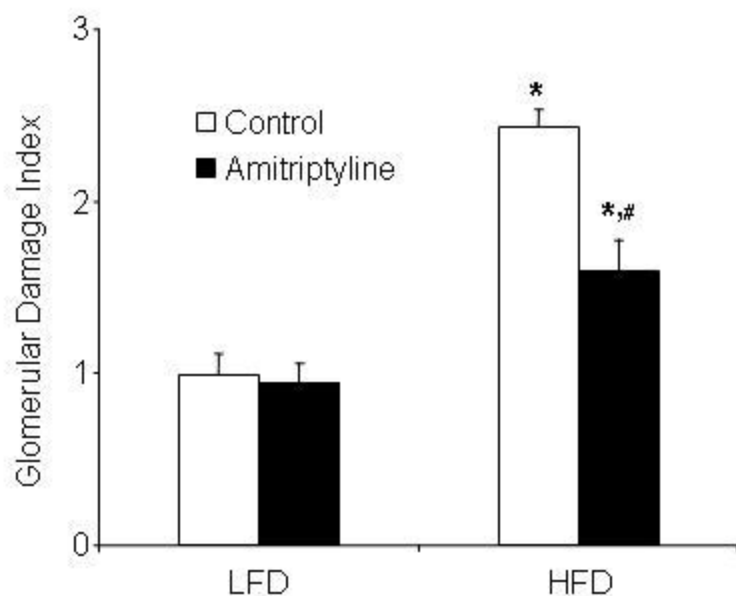


**Fig. 4**

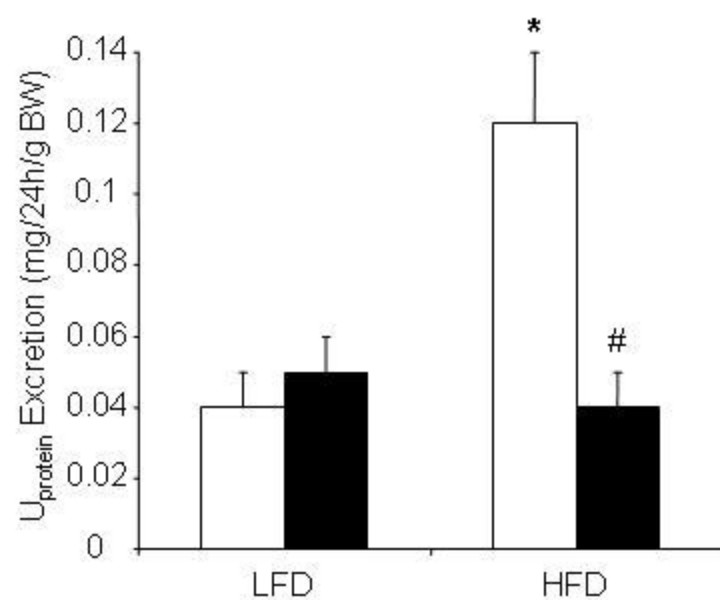
**A**



**B**



**C**



**D**

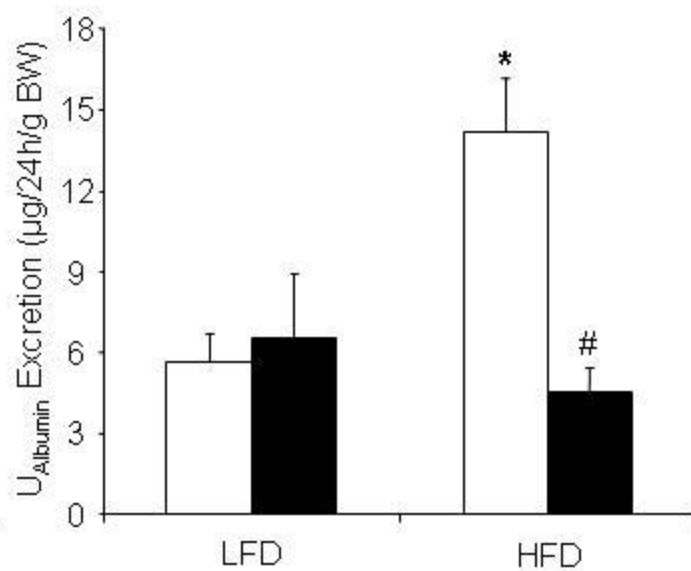
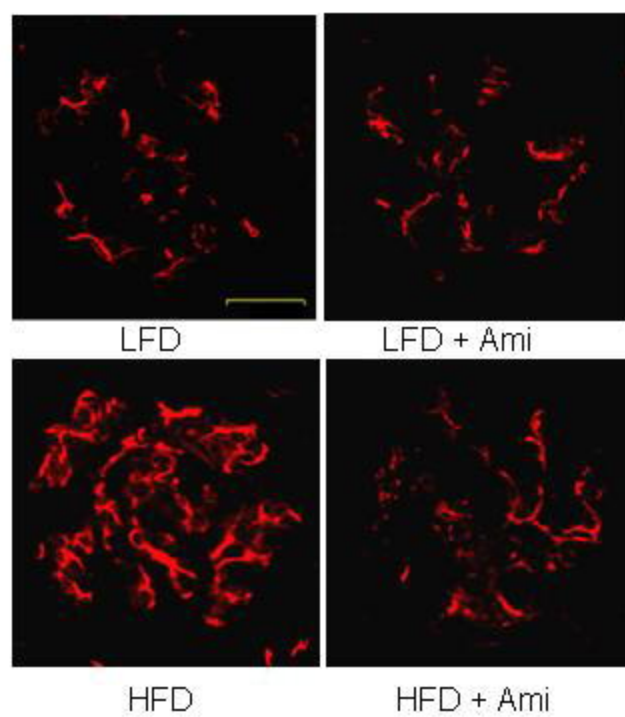




**Fig. 5**

**A**



**B**

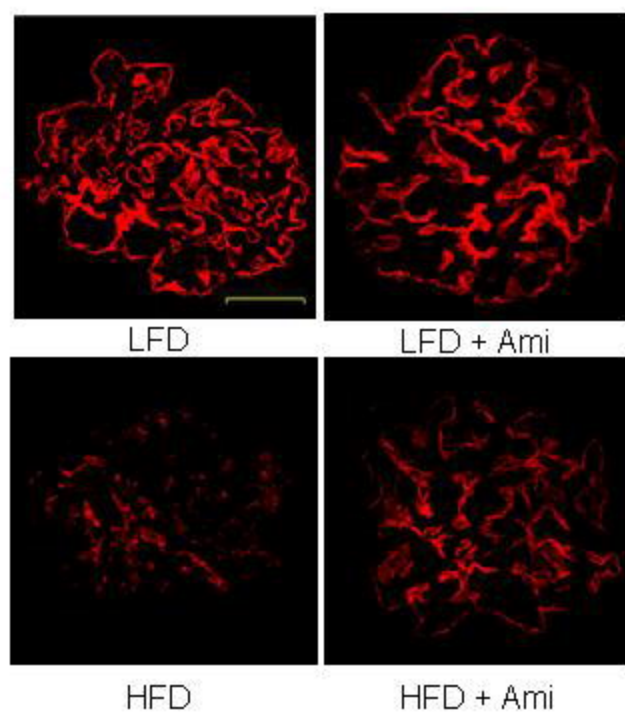


**Fig. 6**

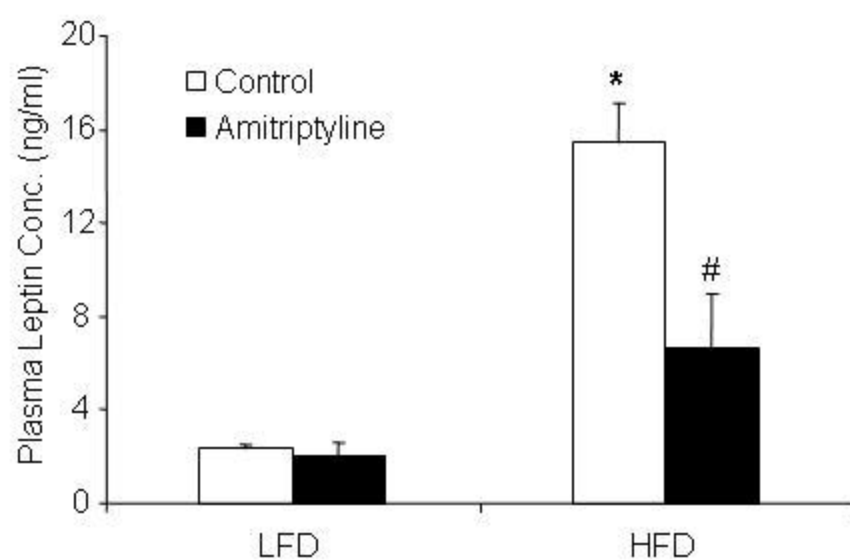
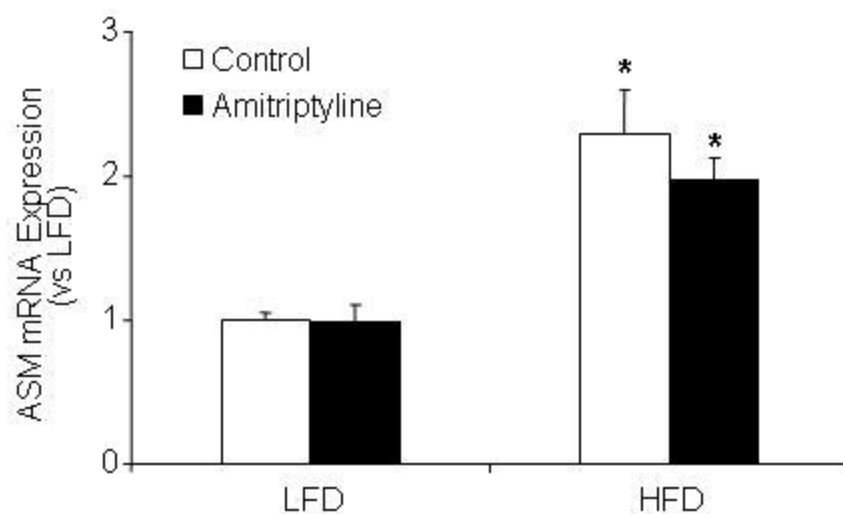


**Fig. 7**

**A**



**B**

